Applicability of the ray theory for *S*-wave propagation in elastic weakly anisotropic inhomogeneous media

Václav Vavryčuk

Geophysical Institute, Czech Academy of Sciences, Boční II/1401, 141 31 Praha 4, Czech Republic

Abstract

Propagation of *P* waves in elastic, weakly anisotropic, inhomogeneous media can be studied by the ray theory without any problem. Propagation of *S* waves in such media, however, creates more complications in the ray theory. These complications are caused mainly by the so-called *S*-wave coupling. It is known that the standard zeroth-order ray theory is inapplicable, if the *S*-wave coupling is significant in the wavefield. In this case, modifications of the ray theory such as the coupling ray theory or the quasi-isotropic approximation of the ray theory have so far been used to reproduce the *S* waves correctly. We show, however, that the failure of the ray theory is not principal, and that it can be overcome even without modifying the ray theory. We show that the ray theory fails because only the zeroth-order term of the ray series is considered. If we include higher-order ray approximations in the solution, we obtain correct results. On a simple example of a plane *S* wave propagating in a weak transversely isotropic medium with a rotating axis of symmetry we study the accuracy of the ray theory in dependence on the number of higher-order ray approximations considered in the ray solution.

Key words: anisotropy, higher-order approximations, inhomogeneity, ray theory, *S*-wave splitting, *S*-wave coupling.

INTRODUCTION

Recently several authors demonstrated that propagation of *S* waves in elastic, weakly anisotropic, inhomogeneous media creates serious complications in the ray theory (Chapman & Shearer 1989; Coates & Chapman 1990; Guest, Thomson & Kendall 1992; Thomson, Kendall & Guest 1992). These complications arise due to the interaction of split *S* waves called "shear-wave coupling". In particular, when polarization vectors of the split *S* waves change rapidly along a ray (e.g., near *S*-wave singularities), and the anisotropy of the medium is weak, the *S*-wave coupling can be quite remarkable, significantly affecting the split *S* waves. In these cases, the standard zeroth-order ray theory can approximate a true solution for the *S* waves very roughly, or it can even yield quite erroneous results. Moreover, the zeroth-order ray solution for an anisotropic medium may not necessarily converge to the zeroth-order ray solution for an isotropic medium, when anisotropy is limiting to isotropy. We can exemplify this surprising and very unwelcome property of the ray theory on the propagation of a plane *S* wave through a vertically inhomogeneous, transversely isotropic medium, for which the inhomogeneity is caused by the symmetry axis of the medium rotating around the vertical axis (see Fig. 1). If a plane *S* wave propagates in the vertical direction, the geometrical ray theory predicts that the polarization of the *S* wave rotates coincidently with the rotation of the symmetry axis (see Fig. 2). The rotation of the *S*-wave polarization is independent of the strength of the anisotropy of the medium. Therefore, when the medium is limiting from anisotropy to isotropy, the ray theory predicts the rotating *S*-wave polarization as the wave propagates along the z-axis. This is obviously an unphysical result, which contradicts the results of the ray theory for an isotropic medium. The "isotropic" ray theory predicts constant *S*-wave polarization, since the above-mentioned medium is homogeneous in the isotropic limit (see Fig. 2). We shall refer to this phenomenon as the "paradox of the ray theory", or as the "failure of the ray theory". An analogous failure of the ray theory can also occur in a strongly anisotropic medium. If we consider a strong transverse isotropy with rotating axis of symmetry and we assume that the deviation of the symmetry axis direction from the vertical axis is infinitely small, then the ray theory also yields contradictory results. In this case, the *S* wave propagates in the *S*-wave singularity direction. Thus the ray theory can fail in weakly as well as in strongly anisotropic media, in the latter case, specifically for the directions near the *S*-wave singularities.

Chapman & Shearer (1989) proposed to overcome the difficulties of the ray theory for anisotropic inhomogeneous media by developing a theory called the "*S*-wave coupling theory". This theory eliminates the failure of the ray theory by calculating the *S*-wave coupling, which is defined as the frequency-dependent interaction between the zeroth-order ray theoretical *S* waves. Coates & Chapman (1990) modified the above-mentioned approach and developed an extension of the asymptotic ray theory called the "coupling ray theory". Pšenčík (1998) and Zillmer, Kashtan & Gajewski (1998) proposed an another modification of the ray theory called the "quasi-isotropic approximation". This theory again tries to take into account the *S*-wave coupling to obtain correct results for *S*-wave propagation in weakly anisotropic inhomogeneous media. All these modifications of the ray theory eliminate the failure of the ray theory, and their results converge smoothly to the results obtained by the ray theory for isotropic media in the case of the limit from anisotropy to isotropy.

In this paper we do not apply any modification of the ray theory in studying S-wave propagation in anisotropic inhomogeneous media. Contrary to the standard zeroth-order ray theory, however, we study the ray solution when higher-order terms of the ray series are considered (Vavryčuk & Yomogida 1996, Vavryčuk 1997). We shall show that the failure of the *zeroth-order ray theory does not necessarily implicate a failure of the higher-order ray theory or the ray theory at all*. We shall show that the quite erroneous results of the zeroth-order ray theory can be satisfactorily corrected by considering the higher-order terms of the ray series. We show that the *S-wave coupling, ignored by the zeroth-order ray approximation, can be reproduced well by the higher-order ray approximations*. Since the problem of propagation of a plane *S* wave through a weakly transversely isotropic medium with a rotating axis of symmetry is simple, we shall try to find the ray solution analytically. Applying the first-order perturbation theory, we shall express explicit analytical formulae for all higher-order approximations of the ray series. Thus we shall obtain an explicit and complete analytical ray solution. This solution is not divergent, as we would expect, but it converges. Moreover, in limiting this solution from anisotropy to isotropy, we obtain results consistent with the results by the isotropic ray theory. On numerical examples we shall study the accuracy of the ray solution by comparing the ray solution with the exact solution obtained by the finite difference method (FD). The accuracy of the ray theory will be studied in dependence on a number of higher-order ray approximations, on the strength of anisotropy of the medium and on the strength of inhomogeneity, meaning the magnitude of the rate of rotation of the symmetry axis of the medium along the *z*-axis.

RAY THEORY FOR ANISOTROPIC INHOMOGENEOUS MEDIA

The elastodynamic equation for an inhomogeneous anisotropic medium, when no sources are considered, reads

$$\rho \ddot{u}_j - \left(\rho a_{ijkl} u_{k,l}\right)_{,i} = 0\,,\ j = 1,2,3 \tag{1}$$

where $\mathbf{u} = \mathbf{u}(\mathbf{x}, t)$ is the displacement, ρ is the density of the medium, a_{ijkl} are the density-normalised elastic parameters, and t is time. We assume that elastic parameters a_{ijkl} and density ρ and their derivatives are continuous functions of coordinates. Solving Eq. (1) using the ray theory (RT) we seek a solution in the form of the ray series (Červený 1972, Eq. 3; Červený, Molotkov & Pšenčík 1977, Eq. 5.2)

$$u_i(\mathbf{x}, t) = \sum_{K=0}^{\infty} U_i^{(K)}(\mathbf{x})\ f^{(K)}(t - \tau(\mathbf{x}))\,, \text{ where } \quad \frac{d}{dt} f^{(K)}(t) = f^{(K-1)}(t)\ . \tag{2}$$

K denotes the order of the ray approximation, $\mathbf{U}^{(K)}(\mathbf{x})$ is the ray amplitude vector, and $\tau(\mathbf{x})$ is the travel time. Eq. (2) describes the ray expansion of only one wave. Since P, S1 or S2 waves can propagate in anisotropic media, the complete solution is obtained by summing the ray expansions of these three waves. Inserting (2) into (1) leads to the system of the *basic equations of the ray theory* for the ray amplitudes $\mathbf{U}^{(K)}$:

$$N_i(\mathbf{U}^{(K)}) - M_i(\mathbf{U}^{(K-1)}) + L_i(\mathbf{U}^{(K-2)}) = 0 \quad , \tag{3}$$

where $\mathbf{N}$, $\mathbf{M}$ and $\mathbf{L}$ are differential operators defined as (Červený 1972, Eq. 6)

$$N_j\left(\mathbf{U}^{(K)}\right) = \Gamma_{jk} U_k^{(K)} - U_j^{(K)}\,,$$

$$M_j\left(\mathbf{U}^{(K)}\right) = a_{ijkl} p_i \frac{\partial U_k^{(K)}}{\partial x_l} + \frac{1}{\rho} \frac{\partial}{\partial x_i}\left(\rho a_{ijkl} p_l U_k^{(K)}\right), \tag{4}$$

$$L_j\left(\mathbf{U}^{(K)}\right) = \frac{1}{\rho} \frac{\partial}{\partial x_i}\left(\rho a_{ijkl} \frac{\partial U_k^{(K)}}{\partial x_l}\right),$$

where $\Gamma_{jk} = a_{ijkl} p_i p_l$ and $p_i = \dfrac{\partial \tau}{\partial x_i}$.

$\mathbf{\Gamma}$ is the Christoffel tensor and $\mathbf{p}$ is the slowness vector. Solving Eq. (3) we obtain the ray amplitude $\mathbf{U}^{(K)}$ as the sum of the additional component $\mathbf{U}^{(K)\perp}$ and the principal component $\mathbf{U}^{(K)\parallel}$:

$$\mathbf{U}^{(K)} = \mathbf{U}^{(K)\perp} + \mathbf{U}^{(K)\parallel}\ , \tag{5}$$

which can be calculated from the system of recursive equations. For the S1-wave expansion we can put (Červený 1972, Eqs 21,22 and 29a,b):

for $K<0$: $U_k^{S1(K)\perp} = U_k^{S1(K)\parallel} = 0$

for $K=0$: $U_k^{S1(0)\perp} = 0$, $U_k^{S1(0)\parallel} = \dfrac{g_k^{S1}}{\sqrt{\rho_0 v_0^{S1} J_0^{S1}}} \sqrt{\rho\, v^{S1} J^{S1}}\, C^{S1(0)}$,

for $K>0$: (6)

$$U_k^{S1(K)\perp} = \left\{ M_i(\mathbf{U}^{S1(K-1)}) - L_i(\mathbf{U}^{S1(K-2)}) \right\} \left\{ \frac{g_i^{S2} g_k^{S2}}{G^{S2}-G^{S1}} + \frac{g_i^{P} g_k^{P}}{G^{P}-G^{S1}} \right\} ,$$

$$U_k^{S1(K)\parallel} = \frac{g_k^{S1}}{\sqrt{\rho_0 v_0^{S1} J_0^{S1}}} \left\{ \sqrt{\rho v^{S1} J^{S1}}\, C^{S1(K)} + \frac{1}{2} \int_{s_0}^{s} \sqrt{\frac{J^{S1}}{\rho v^{S1}}} \left[L_i(\mathbf{U}^{S1(K-1)}) - M_i(\mathbf{U}^{S1(K)\perp}) \right] g_i^{S1} ds \right\} ,$$

where v is the group velocity, J is the ray Jacobian, $\mathbf{g}$ is the polarization vector, G is the eigenvalue of the Christoffel tensor $\mathbf{\Gamma}$, s is the arclength of the ray, and $C^{(K)}$ is the integration constant of the Kth-order ray approximation, which should be determined from the boundary conditions. Quantities with subscript 0 are taken at the initial point of the ray. In Eq. (6) we do not consider phase shifts due to caustics. Analogous equations can be written also for the P- or S2-wave expansions.

WEAK TRANSVERSE ISOTROPY WITH ROTATING AXIS OF SYMMETRY

Let us consider a transversely isotropic medium (TI) with a vertical axis of symmetry. The medium will be described by the following density-normalised elastic parameters (hereafter referred to only as elastic parameters):

a_{11}, a_{44}, a_{66}, $a_{33} = a_{11}$ and $a_{13} = a_{11} - 2a_{44}$, (7)

where the 2-index Voigt notation has been used. This transverse isotropy is very simple and in many aspects similar to isotropy: polarization vectors of *P*, *SV* and *SH* waves are identical to those in isotropic media, and also phase velocities of *P* and *SV* waves are the same as for isotropic media

$c^P = \sqrt{a_{11}}$, $c^{SV} = \sqrt{a_{44}}$. (8)

The only difference between this simple transverse isotropy and isotropy is that the phase velocity of the *SH* wave is directionally dependent having the following form:

$c^{SH} = \sqrt{a_{66} \sin^2 \vartheta + a_{44} \cos^2 \vartheta}$, (9)

where ϑ is the angle between the phase normal and the symmetry axis. For the symmetry axis direction ($\vartheta = 0$), the *SV* and *SH* waves propagate with the same velocity, and form a kiss singularity (Crampin 1991). For other directions, the *SV* and *SH* waves propagate with different velocities, thus splitting into two independent waves. If parameters a_{44} and a_{66} have similar values: $|a_{66} - a_{44}| << a_{44}$, the transverse isotropy becomes weak and the splitting of the *SV* and *SH* waves is not so prominent. Eq. (9) can then be linearized as

$$c^{SH} = \sqrt{a_{44}}\left(1 + \gamma \sin^2 \vartheta\right) \ , \ \text{where } \gamma = \frac{a_{66} - a_{44}}{2a_{44}} \ , \ |\gamma| << 1 \ . \qquad (10)$$

Parameter γ is the well-known Thomsen parameter (Thomsen 1986, Eq. 8b), the other Thomsen parameters ε and δ (Thomsen 1986, Eqs 8a, 17) defining a weak transverse isotropy (WTI) are zero in our case.

The above-mentioned WTI medium will serve to construct the *inhomogeneous anisotropic medium* under study. First, we shall incline the symmetry axis of the WTI medium from the vertical by constant angle ϑ. Second, the axis of symmetry will rotate uniformly around the vertical in dependence on the *z*-coordinate. Thus the unit direction vector of the symmetry axis will be expressed as

$$\mathbf{N} = \mathbf{N}(z) = \begin{bmatrix} \cos\vartheta \cos\varphi(z) \\ \cos\vartheta \sin\varphi(z) \\ \sin\vartheta \end{bmatrix} , \qquad (11)$$

where ϑ is the deviation of the symmetry axis from the vertical, $\varphi = bz$ is the angle of rotation of the symmetry axis which is measured in the *x*-*y* plane, and *b* is the parameter expressing the rate of rotation of the symmetry axis along the *z*-axis.

In this way we obtain a vertically inhomogeneous WTI medium called the *WTI medium with a rotating axis of symmetry.* The expressions for the elastic parameters a'_{ij} of this medium are given in the Appendix. The density of the medium is constant.

PROPAGATION OF PLANE *S* WAVES ALONG THE Z-AXIS BY RT

In this section we shall study the properties of plane *S* waves propagating in the above-defined medium along the *z*-axis by applying the ray theory. The wave will propagate from *z*=0 in the positive direction. At the initial point, *z*=0, the *S* wave will be linearly polarised in the direction of the *x*-axis and will have the form of the Dirac delta function. In the ray theory, the studied *S* wave is composed of two elementary *S* waves: *S*1 and *S*2. Both *S* waves are polarised in the *x*-*y* plane. Hereafter we shall not distinguish these two elementary *S* waves by their arrival times, but rather by their polarization. Therefore, we shall not use the notation *S*1 and *S*2 waves, but the notation *SR* (radial *S*) and *ST* (transverse *S*) waves. The *SR* wave will be the elementary *S* wave, whose principal component is parallel to the projection of the symmetry axis of WTI in the *x-y* plane. The *ST* wave will be that elementary *S* wave, whose principal component is perpendicular to the projection of the symmetry axis of WTI in the *x-y* plane (see Fig. 3). We shall now try to express analytically the zeroth-order ray approximation and all the higher-order terms of the ray expansions of these waves.

Rayfields and ray Jacobians of the SR and ST waves

Rayfields of the *SR* and *ST* waves are different. For the *SR* wave, the rayfield is very simple. Since the phase and group velocity vectors of this wave are constant and do not depend on the symmetry axis direction, the rays are straight lines parallel to the phase normal, and the ray Jacobian is unit:

$$c^{SR} = v^{SR} = \sqrt{a_{44}}\ , \ J^{SR} = 1\,, \tag{12}$$

where c^{SR} and v^{SR} are the phase and group velocities of the *SR* wave. and J^{SR} is the ray Jacobian.

For the *ST* wave, the rayfield is more complicated. Since the deviation between the phase normal and the symmetry axis of WTI is constant, the magnitude of the group velocity of the *ST* wave is also constant for all points at the ray. However, the group velocity direction depends on the symmetry axis direction that rotates along the z-axis. It results in rays forming a circular helix (see Fig. 4):

$$x = r_0 \sin\varphi + x_0\,,\ y = r_0 \cos\varphi + y_0\,,\ z = c^{ST} t = b^{-1}\varphi\ \text{, where } r_0 = b^{-1}\sin\delta\ , \tag{13}$$

where x_0 and y_0 are ray parameters, φ is the monotonically increasing angle of rotation of the symmetry axis of WTI, b is the rate of rotation, c^{ST} is the phase velocity of the *ST* wave, and δ is the angle between the z-axis and the ray. Phase and group velocities c^{ST} and v^{ST}, and deviation δ can be approximately expressed in WTI as follows:

$$c^{ST} = v^{ST} = \sqrt{a_{44}}\left(1 + \gamma \sin^2\vartheta\right),\ \sin\delta = 2\gamma \sin\vartheta \cos\vartheta\,, \tag{14}$$

where γ is the Thomsen parameter defined by Eq. (10) and ϑ is the angle between the *z*-axis and the symmetry axis of WTI. Similarly to the *SR* wave, the ray Jacobian is constant and unit:

$$J^{ST} = 1\,. \tag{15}$$

We emphasise that, contrary to the *SR* wave to which Eq. (12) holds exactly, Eqs (14) and (15) for the *ST* wave are approximate being valid only under a weak anisotropy condition.

Zeroth-order ray approximation

Taking into account Eqs (6), (12) and (15), we can express the zeroth-order ray approximation of the *SR* and *ST* waves as:

$$u_k^{SR(0)}(\mathbf{x},t) = C^{SR(0)\|} g_k^{SR} \delta\left(t - \frac{z}{c^{SR}}\right),\; u_k^{ST(0)}(\mathbf{x},t) = C^{ST(0)\|} g_k^{ST} \delta\left(t - \frac{z}{c^{ST}}\right), \tag{16}$$

where $\mathbf{g}^{SR} = \begin{bmatrix} \cos\varphi \\ -\sin\varphi \\ 0 \end{bmatrix}$, $\mathbf{g}^{ST} = \begin{bmatrix} \sin\varphi \\ \cos\varphi \\ 0 \end{bmatrix}$, and $\varphi = bz$.

From (16) we can see that polarization of the *SR* and *ST* waves rotates in coincidence with the rotation of the symmetry axis of WTI. This rotation is independent of the strength of the anisotropy controlled by the Thomsen parameter γ.

Higher-order ray approximations

Using Eq. (16) for the zeroth-order ray approximation and Eq. (6) for the higher-order terms of the ray expansion, we can recursively calculate the whole ray series for the *SR* and *ST* waves. Although the medium is very simple and we are studying the propagation of a plane wave, the procedure of analytical calculation of higher-order ray approximations involves extensive manipulation with rather complex formulae. Therefore, we performed the calculations by using the symbolic manipulation software REDUCE (Hearn 1991). In this section, we shall not present a detailed derivation, but only the final formulae.

The basic problem in calculating the higher-order ray approximations is to determine the zeroth- and higher-order integration constants. The integration constants should be determined from the boundary conditions imposed on the *S* wave at $z = 0$. Since the incident *S* wave has the form of the Dirac delta function polarized in the *x*-axis

$$\mathbf{u}^S(z = 0, t) = (\delta(t),\ 0,\ 0)^T \tag{17}$$

we can conclude from (16) that

$$c^{SR(0)\|} = 1 \quad \text{and} \quad c^{ST(0)\|} = 0\ . \tag{18}$$

The higher-order integration constants of the *SR* and *ST* waves are determined from the following equation:

$$\sum_{K=1}^{\infty} \left[\mathbf{u}^{(K)SR}(z = 0, t) + \mathbf{u}^{(K)SR}(z = 0, t)\right] = 0\,, \tag{19}$$

expressing the fact that the higher-order ray approximations of the *SR* and *ST* waves cancel each other at $z = 0$. The sum of the higher-order ray approximations of the *SR* and *ST* waves

(19) will hereafter be referred to as the *complete higher-order ray solution*. Obviously, if Eqs (18) and (19) are satisfied, the boundary conditions are also satisfied. Since function $f^{(K)}(t)$ from Eq. (2) has the form

$$f^{(0)}(t)=\delta(t) \text{ and } f^{(K)}(t)=\frac{t^{K-1}}{(K-1)!}H(t) \text{ for } K>0\,, \tag{20}$$

Eq. (19) can be expressed as

$$\sum_{K=1}^{\infty}\left[U^{(K)SR\parallel}(z=0)+U^{(K)ST\perp}(z=0)\right]t^K=0\,,$$

$$\sum_{K=1}^{\infty}\left[U^{(K)SR\perp}(z=0)+U^{(K)ST\parallel}(z=0)\right]t^K=0\,. \tag{21}$$

Eq. (21) should be valid for all times t, and can thus be decomposed into a system of recursive equations for the higher-order integration constants:

$$U^{(K)SR\parallel}(0)+U^{(K)ST\perp}(0)=0\,,$$

$$U^{(K)SR\parallel}(0)+U^{(K)ST\perp}(0)=0\,. \tag{22}$$

where $K>0$. Using Eq. (22) we can express the integration constants as follows:

$$C^{ST(K)}=2\frac{1+2K}{1+K}\left(\frac{\sqrt{a_{44}}b}{\gamma\sin^2\vartheta}\right)^K\left[1+(1+3K)\gamma\sin^2\vartheta\right],\ C^{SR(K)}=0, \quad \text{for } K=1,3,5,7,\ldots\,,$$

$$C^{ST(K)}=0,\ C^{SR(K)}=\frac{1+2K}{1+K}\left(\frac{\sqrt{a_{44}}b}{\gamma\sin^2\vartheta}\right)^K\left[1+3K\gamma\sin^2\vartheta\right], \quad \text{for } K=0,2,4,6,\ldots\,. \tag{23}$$

Thus, we obtain the final formulae for the ray series for the SR and ST waves:

$$u_i^{ST}(\mathbf{x},t)=U_i^{ST(0)}\delta\left(t-\tau^{ST}\right)+\sum_{K=0}^{\infty}U_i^{ST(K+1)}\frac{\left(t-\tau^{ST}\right)^K}{K!}H\left(t-\tau^{ST}\right),$$

$$u_i^{SR}(\mathbf{x},t)=U_i^{SR(0)}\delta\left(t-\tau^{SR}\right)+\sum_{K=0}^{\infty}U_i^{SR(K+1)}\frac{\left(t-\tau^{SR}\right)^K}{K!}H\left(t-\tau^{SR}\right), \tag{24}$$

with ray amplitudes $\mathbf{U}^{SR(K)}$ and $\mathbf{U}^{ST(K)}$ expressed as follows:

$$U_i^{SR(K)}=U^{SR(K)\parallel}g_i^{SR}+U^{SR(K)\perp}g_i^{ST},\ U_i^{ST(K)}=U^{ST(K)\parallel}g_i^{ST}+U^{ST(K)\perp}g_i^{SR}, \tag{25}$$

where

for K=0: $U^{ST(0)\parallel}=U^{ST(0)\perp}=0$, $U^{SR(0)\parallel}=1$, $U^{SR(0)\perp}=0$,

for K>0:

$$U^{SR(K+1)\parallel} = \left(1+\frac{1}{2}(3K+3)\gamma \sin^2 \vartheta\right)\left(\frac{b\sqrt{a_{44}}}{\gamma \sin^2 \vartheta}\right)^{K+1} K! \sum_{N=0}^{N\le\frac{K+1}{2}} \frac{\varphi^{K-2N+1}}{N!(K-N)!\,(K-2N+1)!} ,$$

$$U^{SR(K+1)\perp} = \left(1+\frac{1}{2}(3K+2)\gamma \sin^2 \vartheta\right)\left(\frac{b\sqrt{a_{44}}}{\gamma \sin^2 \vartheta}\right)^{K+1} K! \sum_{N=0}^{N\le\frac{K}{2}} \frac{\varphi^{K-2N}}{N!(K-N)!\,(K-2N)!} , \tag{26}$$

$$U^{ST(K+1)\parallel} = (-1)^K\left(1+\frac{1}{2}(3K+2)\gamma \sin^2 \vartheta\right)\left(\frac{b\sqrt{a_{44}}}{\gamma \sin^2 \vartheta}\right)^{K+1} K! \sum_{N=0}^{N\le\frac{K}{2}} \frac{\varphi^{K-2N}}{N!(K-N)!\,(K-2N)!} ,$$

$$U^{ST(K+1)\perp} = (-1)^K\left(1+\frac{1}{2}(3K+3)\gamma \sin^2 \vartheta\right)\left(\frac{b\sqrt{a_{44}}}{\gamma \sin^2 \vartheta}\right)^{K+1} K! \sum_{N=0}^{N\le\frac{K-1}{2}} \frac{\varphi^{K-2N-1}}{N!(K-N)!\,(K-2N-1)!} .$$

Traveltimes τ^{SR} and τ^{ST} in (24) are expressed as follows

$$\tau^{SR} = \frac{z}{\sqrt{a_{44}}} \text{ and } \tau^{ST} = \frac{z}{\sqrt{a_{44}}}\left(1-\gamma \sin^2 \vartheta\right) . \tag{27}$$

Limit from anisotropy to isotropy

The complete higher-order RT solution (19) that is identically zero at $z=0$ has special properties also for other z. It can be shown that for $z>0$ the higher-order RT solution is non-zero only for the times between the arrivals of the *SR* and *ST* waves. For times outside this time interval, the *S* wave is identically zero. If the anisotropy is very weak, the difference between the arrival times of the split *S* waves is very small and the non-zero amplitudes are concentrated in a very narrow time interval. With decreasing width of this time interval, the amplitude of the higher-order RT solution increases. For vanishing anisotropy, the width of the time interval vanishes and the waveform of the higher-order RT solution becomes the Dirac delta function similarly to the zeroth-order RT solution. Thus the complete RT solution in the limit from anisotropy to isotropy can be expressed as

$$\mathbf{u}^{iso}(z,t) \equiv \lim_{\gamma\to 0} \mathbf{u}(z,t) = \mathbf{U}^{iso}(z)\,\delta\left(t-\frac{z}{\sqrt{a_{44}}}\right) , \tag{28}$$

where amplitude $\mathbf{U}^{iso}(z)$ can be calculated as the sum of the zeroth-order ray amplitude and the time integral of the higher-order RT solution of the faster *S* wave over the time interval between the *SR*- and *ST*-wave arrivals. If anisotropy parameter γ is positive, the faster wave is the *ST* wave and amplitude $\mathbf{U}^{iso}(z)$ can be expressed as follows:

$$\mathbf{U}^{iso}(z)=\mathbf{g}^{SR}+\lim_{\gamma\to 0}\int_{\tau^{ST}}^{\tau^{SR}}\mathbf{u}^{ST}(z,t)dt=\mathbf{g}^{SR}+\lim_{\gamma\to 0}\sum_{K=1}^{\infty}\left[\left(\mathbf{g}^{ST}U^{ST(K)\parallel}+\mathbf{g}^{SR}U^{ST(K)\perp}\right)\frac{1}{(K-1)!}\int_{\tau^{ST}}^{\tau^{SR}}\left(t-\tau^{ST}\right)^{K-1}dt\right]=$$

$$=\mathbf{g}^{ST}\lim_{\gamma\to 0}\sum_{K=1}^{\infty}\left[\frac{1}{K!}U^{ST(K)\parallel}\left(\tau^{SR}-\tau^{ST}\right)^{K}\right]+\mathbf{g}^{SR}\left\{1+\lim_{\gamma\to 0}\sum_{K=1}^{\infty}\left[\frac{1}{K!}U^{ST(K)\perp}\left(\tau^{SR}-\tau^{ST}\right)^{K}\right]\right\}. \tag{29}$$

Taking into account that

$$\tau^{SR}-\tau^{ST}=\frac{\gamma\sin^2\vartheta}{b\sqrt{a_{44}}}\varphi\ , \tag{30}$$

and using Eq. (26), we obtain

$$\lim_{\gamma\to 0}\sum_{K=0}^{\infty}\left\{\frac{1}{K!}U^{ST(K)\parallel}\left(\tau^{SR}-\tau^{ST}\right)^{K}\right\}=\sum_{K=0}^{\infty}(-1)^K\frac{\varphi^{2K+1}}{(2K+1)!}=\sin\varphi\,,$$

$$1+\lim_{\gamma\to 0}\sum_{K=0}^{\infty}\left\{\frac{1}{K!}U^{ST(K)\perp}\left(\tau^{SR}-\tau^{ST}\right)^{K}\right\}=\sum_{K=0}^{\infty}(-1)^K\frac{\varphi^{2K}}{(2K)!}=\cos\varphi\,. \tag{31}$$

Thus $\mathbf{U}^{iso}(z,t)=(1,\ 0,\ 0)^T$ and the final formula for the complete RT solution in the isotropic limit $\mathbf{u}^{iso}(z,t)$ is expressed as follows

$$\mathbf{u}^{iso}(z,t)=(1,\ 0,\ 0)^T\,\delta\left(t-\frac{z}{\sqrt{a_{44}}}\right). \tag{32}$$

Obviously, we found a true solution. In a homogeneous isotropic medium, the plane *S* wave propagates with a constant amplitude and is polarized identically as the incident *S* wave independently of the *z*-coordinate. A similar result is obtained for a negative anisotropy parameter γ , when the faster wave is the *SR* wave.

PROPAGATION OF PLANE *S* WAVES ALONG THE *Z*-AXIS BY FD

In this section, we shall solve the same problem as in the previous section but using the finite difference method. Since we are considering a vertically inhomogeneous medium in which a plane wave propagates along the *z*-axis, displacement **u** will depend only on the z-coordinate, $\mathbf{u}=\mathbf{u}(z,t)$, and equation (1) simplifies to

$$\ddot{u}_1-\left(a_{55}u_{1,3}+a_{45}u_{2,3}\right)_{,3}=0\ ,\ \ddot{u}_2-\left(a_{45}u_{1,3}+a_{44}u_{2,3}\right)_{,3}=0\ , \tag{33a}$$

$$\ddot{u}_3-\left(a_{33}u_{3,3}\right)_{,3}=0\,. \tag{33b}$$

Both equations (33a) and (33b) are independent. Equation (33a) represents a system of two coupled partial differential equations describing the propagation of plane *S* waves. Equation (33b) describes the propagation of a plane *P* wave. Since parameter a_{33} is constant (see

Appendix), the plane P wave behaves in the same way as in a homogeneous isotropic medium. Equation (33a) can be expressed as a system of four first-order partial differential equations

$$\dot{v}_1 = t_1{,}_3 \; \dot{v}_2 = t_2{,}_3 \ ,$$

$$\dot{t}_1 = a_{55}v_1{,}_3 + a_{45}v_2{,}_3 \, , \; \dot{t}_2 = a_{45}v_1{,}_3 + a_{44}v_2{,}_3 \, , \tag{34}$$

where v_1 and v_2 are the horizontal components of the velocity, and t_1 and t_2 are components of the density-normalised stress tensor. We can express Eq. (34) in a more compact matrix form as

$$\frac{d}{dt}\mathbf{y} = \mathbf{A}\frac{d}{dz}\mathbf{y} \, , \tag{35}$$

where

$$\mathbf{A} = \begin{bmatrix} 0 & 0 & 1 & 0 \\ 0 & 0 & 0 & 1 \\ a_{55} & a_{45} & 0 & 0 \\ a_{45} & a_{44} & 0 & 0 \end{bmatrix} , \; \mathbf{y} = \begin{bmatrix} v_1 \\ v_2 \\ t_1 \\ t_2 \end{bmatrix} .$$

This equation is a time-domain version of the matrix equation used by Woodhouse (1974, Eq. 2.9), Fryer & Frazer (1984, Eq, 2.1) or Chapman (1994, Eq. 6), which is further simplified by considering the TI medium with a rotating axis of symmetry and by confining oneself only to the vertical direction of wave propagation.

Converting the derivatives in (35) into finite differences by using the standard *central-difference* formulae of second-order accuracy (Aki & Richards 1980, p. 775) and using the *explicit* scheme, we obtain the *system of finite-difference equations* in the following form:

$$\mathbf{y}(t+\Delta t, z) = \Delta t \left[\mathbf{A}\frac{\mathbf{y}(t, z+\Delta z) - \mathbf{y}(t, z-\Delta z)}{\Delta z} + \mathbf{y}(t-\Delta t, z) \right] , \tag{36}$$

where Δt and Δz are the time and space steps, which should satisfy the *stability condition*:

$$\Delta t \le \frac{\Delta z}{v^S} \ . \tag{37}$$

v^S denotes the maximum value of the S-wave group velocity. The size of the finite-difference model will be chosen in such a way that the studied wavefield will not be affected by the waves reflected from the boundary. Therefore, we can apply the simplest boundary conditions by specifying the *rigid boundary*. The S wave propagating in the model will be initiated by applying the non-zero *initial conditions* at z=0.

NUMERICAL EXAMPLE

In this section, we shall give a numerical example of applying the ray-theoretical formulae derived in previous sections. We shall calculate the RT solution for a number of higher-order ray approximations and compare then with the exact solution obtained by the FD method.

Accordingly to previous sections, we shall assume that the incident plane *S* wave is polarized at *z*=0 along the *x*-axis thus being the pure *SR* wave at *z*=0. The incident *S* wave will have a unit amplitude, and the waveform will be a one-sided pulse expressed as

$$\mathbf{u}(z=0,t)=\left(\sin^2\left(\frac{\pi t}{T}\right),\ 0,\ 0\right)^T \text{ for } t\in<0,T> . \qquad (38)$$

For other times, $\mathbf{u}(z=0,t)$ will be zero. For parameter *T* specifying the pulse width, we use the value *T*=1s.

The *S* wave will propagate in two models of an anisotropic medium. The first model is called the "weak anisotropy" model and is specified by values $a_{44}=6.00$ and $\gamma=0.15$. The second model is called the "very weak anisotropy" model being specified by values $a_{44}=6.00$ and $\gamma=0.003$. The latter model displays 50 times weaker anisotropy than the first model, thus almost approaching an isotropic medium. Note that we do not need to specify parameter a_{11} for the *S*-wave propagation. For the rate of rotation of the symmetry axis we use values *b*=0.032, 0.064, 0.096 and 0.128, that correspond to the rotation of the symmetry axis through angle $\varphi=\pi$ over distances $z=40\lambda^{SR}$, $20\lambda^{SR}$, $13.3\lambda^{SR}$ and $10\lambda^{SR}$, where λ^{SR} denotes the wavelength of the incident *S* wave, $\lambda^{SR}=c^{SR}T=\sqrt{a_{44}}T=2.45$ km.

The *S* wave propagating in the above-mentioned media will be calculated using the ray method by formulae (24)-(26) and using the FD method by formula (36). In the FD calculations we have used the following values of the space and time steps: $\Delta z=0.02$ km and $\Delta t=0.004$ s.

Figure 5 shows a comparison of the zeroth-order RT solution with the exact solution for four receivers in the weak and very weak anisotropy models. We can see from the left-hand diagrams that the incident *S* wave is polarized at *z*=0 along the *x*-axis, thus being the pure *SR* wave. As the wave propagates through the medium, the exact waveforms and particle motions (Fig. 5, solid line) change. The changes are more distinct for weak anisotropy than for very weak anisotropy. In very weak anisotropy, the predominant *S*-wave polarization remains unchanged, and the ellipticity of the wave increases only slightly. In weak anisotropy, however, the ellipticity of the *S* wave is approximately constant, but the predominant polarization direction rotates in coincidence with the rotation of the symmetry axis of the medium. For the most distant receiver (right-hand diagrams) we observe the forming of an another *S* wave, which is faster having a smaller amplitude and being polarized perpendicularly to the polarization of the predominant and slower *S* wave.

For both anisotropy models, the zeroth-order ray theory predicts the same results (Fig. 5, dashed line): the propagating *S* wave is a pure *SR* wave for all receivers, it is linearly polarized and it has a unit amplitude. In the weak anisotropy model, polarization of the zeroth-order RT wave coincides with the predominant polarization direction of the exact *S* wave. In the very weak anisotropy model, however, the waveforms and particle motions of the *zeroth-order RT solution are drastically different from the exact solution*. Therefore, the zeroth-order ray theory fails totally in this case.

Figure 6 shows the behavior of the RT solution when higher-order ray approximations are considered. Waveforms and particle motions are shown for the receiver at $z = 13.3\lambda^{SR}$. For both anisotropy models, the fit between the exact and RT solutions improves rapidly if the higher-order ray approximations are included. The more approximations we consider, the better fit we obtain. For the configuration used, the six higher-order ray approximations are sufficient to reproduce the exact solution within the width of the line.

Figure 7 displays the comparison of the exact and RT solutions for anisotropy models with a different rate of symmetry axis rotation. The waveforms and particle motions are displayed for the receiver at $z = 6.6\lambda^{SR}$. The rate of the symmetry axis rotation increases in the diagrams from left to right. Comparing the diagrams with the different rates of rotation, we observe that the fit between the exact and RT solutions decreases with increasing rate of rotation. Therefore, for higher rates of rotation we have to consider a higher number of ray approximations to obtain a solution of reasonable accuracy. Specifically, for the rate of rotation $b = \pi / 10\lambda^{SR}$, the differences between the exact solution and the RT solution with 7 higher-order ray approximations are quite large for both anisotropy models. But the RT solution with 10 higher-order approximations coincides with the exact solution quite well (within the width of the line).

CONCLUSION

In this paper we have demonstrated that the *ray theory is applicable even for S waves propagating in weakly anisotropic, inhomogeneous media*. The propagation of a plane *S* wave in a weakly transversely isotropic medium with rotating axis of symmetry was used as an example to show that the *zeroth-order ray-theoretical solution can totally fail, but the whole ray series can converge to the true solution*. This is of particular interest, because it is usually assumed that when the zeroth-order ray theory fails, the whole ray series will also fail. We have proved that the *S*-wave coupling introduced by Chapman & Shearer (1989) and by Coates & Chapman (1990) and ignored by the zeroth-order ray theory, can be successfully reproduced by the higher-order ray theory. Comparing the ray solution with the exact solution calculated by the FD method, we have proved that the accuracy of the ray solution increases with the number of higher-order ray approximations considered. This observation is valid even for very weak anisotropy almost approaching isotropy. On the contrary, the accuracy decreases when the rate of rotation of the symmetry axis of the medium increases. For high values of the rate of rotation, the medium becomes strongly inhomogeneous, and the zeroth-order ray theory is inapplicable, because the elastic properties of the medium change significantly over distances comparable with the predominant wavelength of the propagating wave. However, if we include the higher-order ray approximations, we can obtain correct results. This implies that a weak inhomogeneity of a medium is not an ultimate condition for the applicability of the ray theory as is commonly assumed. It seems that the weak inhomogeneity condition is bound only to the zeroth-order ray theory. We should stress, however, that for a strong inhomogeneity, the number of higher-order ray approximations having to be considered can be fairly high and thus computationally unrealizable. Furthermore, we observed that the accuracy of the ray solution decreases with increasing length of the ray of the propagating *S* wave. For more distant observers, we have to include more higher-order ray approximations to obtain a comparable accuracy for all receivers. Hypothetically, for very distant observers we have to apply an almost infinite number of higher-order ray approximations to obtain satisfactory results.

The conclusions made for weak transverse isotropy are valid also for strong transverse isotropy, if the *S* wave propagates near a kiss singularity. This occurs if the deviation between the rotating axis of symmetry and the vertical axis is small. If we limit this deviation to zero, the zeroth-order ray solution fails, but considering a sufficiently high number of higher-order ray approximations yields correct results.

Finally, we have to mention that for simplicity we studied the *S*-wave propagation in an extremely simple and in many aspects unrealistic structure. We did not discuss the aspects of computing the higher-order ray approximations in more realistic anisotropic and inhomogeneous media. Therefore, the paper should be viewed as a contribution to a general understanding of the problem of applicability of the higher-order ray theory rather than as an instruction how to apply the higher-order ray theory to modeling the *S* wavefield in realistic situations. It can be expected that in many cases, when the higher-order ray theory works in principle, it need not to be practical or efficient or even possible to apply it in numerical computations. Nevertheless, it seems that further development of the higher-order ray theory, in particular, the development of its computing aspects, would be desirable.

References

Aki, K. & P. G. Richards, 1980. *Quantitative Seismology. Theory and Methods* II, W. H. Freeman, San Francisco.

Červený, V., 1972. Seismic rays and ray intensities in inhomogeneous anisotropic media, *Geophys. J. Roy. Astr. Soc.*, **29**, 1-13.

Červený, V., Molotkov, I. & I. Pšenčík, 1977. *Ray Method in Seismogy*, Charles University Press, Prague.

Chapman, C. H., 1994. Reflection/transmission coefficient reciprocities in anisotropic media, *Geophys. J. Int.*, **116**, 498-501.

Chapman, C. H. & P. M. Shearer, 1989. Ray tracing in azimuthally anisotropic media – II. Quasi-shear wave coupling, *Geophys. J.* , **96**, 65-83.

Coates, R. T. & C. H. Chapman, 1990. Quasi-shear wave coupling in weakly anisotropic 3-D media, *Geophys. J. Int.*, **103**, 301-320.

Crampin, S., 1991. Effects of point singularities on shear-wave propagation in sedimentary basins, *Geophys. J. Int.*, **107**, 531-543.

Fryer, G. J. & L. N. Frazer, 1984. Seismic waves in stratified anisotropic media, *Geophys. J. Roy. Astr. Soc.*, **78**, 691-710.

Guest, W. S., Thomson, C. J. & J-M. Kendall, 1992. Displacement and rays for splitting *S*-waves: perturbation theory and the failure of the ray method, *Geophys. J. Int.*, **108**, 372-378.

Hearn, A. C., 1991. *REDUCE 3.4. User's Manual*. RAND Corporation, Santa Monica.

Pšenčík, I., 1998. Green functions for inhomogeneous weakly anisotropic media, *Geophys. J. Int.*, in print.

Thomsen, L., 1986. Weak elastic anisotropy, *Geophysics*, **51**, 1954-1966.

Thomson, C. J., J-M. Kendall & W.S. Guest, 1992. Geometrical theory of shear-wave splitting: corrections to ray theory for interference in isotropic/anisotropic transitions, *Geophys. J. Int.*, **108**, 339-363.

Vavryčuk, V., 1997. Elastodynamic and elastostatic Green tensors for homogeneous weak transversely isotropic media, *Geophys. J. Int.*, **130**, 786-800.

Vavryčuk, V. & Yomogida, K., 1996. *SH*-wave Green tensor for homogeneous transversely isotropic media by higher-order approximations in asymptotic ray theory, *Wave Motion*, **23**, 83-93.

Woodhouse, J. H., 1974. Surface waves in a laterally varying layered structure, *Geophys. J. Roy. Astr. Soc.*, **37**, 461-490.

Zillmer, M., Kashtan, B. M. & D. Gajewski, 1998. Quasi-isotropic approximation of anisotropic ray theory, *Geophys. J. Int.*, **132**, 643-653.

Appendix – Elastic parameters of the WTI medium with rotating axis of symmetry

Elastic parameters a'_{ij} of the WTI medium with rotating axis of symmetry can be expressed by elastic parameters a_{11}, a_{44} and γ of the WTI medium, for which the axis of symmetry coincides with the vertical axis (see Eqs 7 and 10), as follows:

$$a'_{11} = a_{11} + 8a_{44}\gamma\cos^2\vartheta\,\sin^2\varphi\,\cos^2\varphi\,, \qquad a'_{12} = a_{11} - 2a_{44} - 8a_{44}\gamma\cos^2\vartheta\,\sin^2\varphi\,\cos^2\varphi\,,$$

$$a'_{13} = a_{11} - 2a_{44}\,, \qquad a'_{14} = 4a_{44}\gamma\sin\vartheta\,\cos\vartheta\,\sin\varphi\,\cos^2\varphi\,,$$

$$a'_{15} = 4a_{44}\gamma\sin\vartheta\,\cos\vartheta\,\sin^2\varphi\,\cos\varphi\,, \qquad a'_{16} = 4a_{44}\gamma\cos^2\vartheta\,\sin\varphi\,\cos\varphi\left(1-2\sin^2\varphi\right),$$

$$a'_{22} = a_{11} + 8a_{44}\gamma\cos^2\vartheta\,\sin^2\varphi\,\cos^2\varphi\,, \qquad a'_{23} = a_{11} - 2a_{44}\,,$$

$$a'_{24} = -4a_{44}\gamma\sin\vartheta\,\cos\vartheta\,\sin\varphi\,\cos^2\varphi\,, \qquad a'_{25} = -4a_{44}\gamma\sin\vartheta\,\cos\vartheta\,\sin^2\varphi\,\cos\varphi\,,$$

$$a'_{26} = -4a_{44}\gamma\cos^2\vartheta\,\sin\varphi\,\cos\varphi\left(1-2\sin^2\varphi\right), \; a'_{33} = a_{11}\,, \;\; a'_{34} = 0\,, \;\; a'_{35} = 0\,, \;\; a'_{36} = 0\,,$$

$$a'_{44} = a_{44} + 2a_{44}\gamma\sin^2\vartheta\,\cos^2\varphi\,, \qquad a'_{45} = 2a_{44}\gamma\sin^2\vartheta\,\sin\varphi\,\cos\varphi\,,$$

$$a'_{46} = 2a_{44}\gamma\sin\vartheta\,\cos\vartheta\,\cos\varphi\left(1-2\sin^2\varphi\right), \qquad a'_{55} = a_{44} + 2a_{44}\gamma\sin^2\vartheta\,\sin^2\varphi\,,$$

$$a'_{56} = 2a_{44}\gamma\sin\vartheta\,\cos\vartheta\,\sin\varphi\,\left(1-2\sin^2\varphi\right), \quad a'_{66} = a_{44} + 2a_{44}\gamma\cos^2\vartheta\,\left(1-4\sin^2\varphi\,\cos^2\varphi\right).$$

TI with rotating axis of symmetry

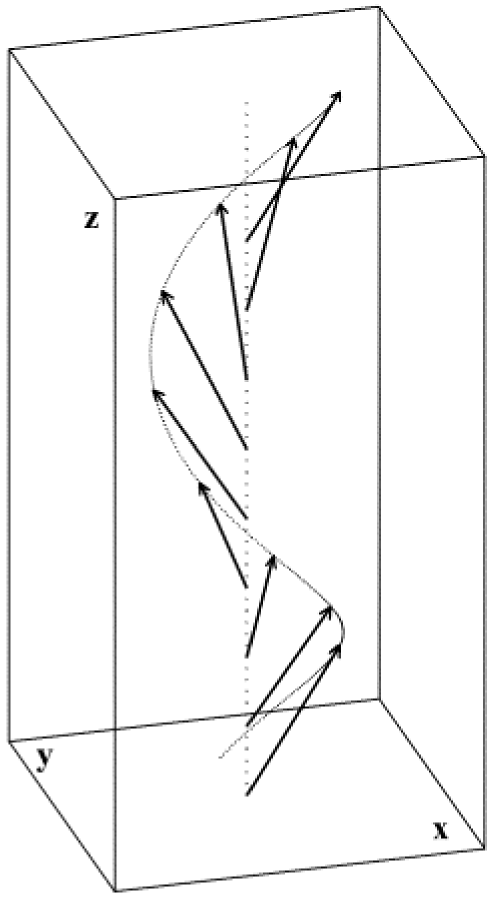

Figure 1. Vertically inhomogeneous transversely isotropic medium. Direction of the symmetry axis depends on the z-coordinate rotating around the z-axis.

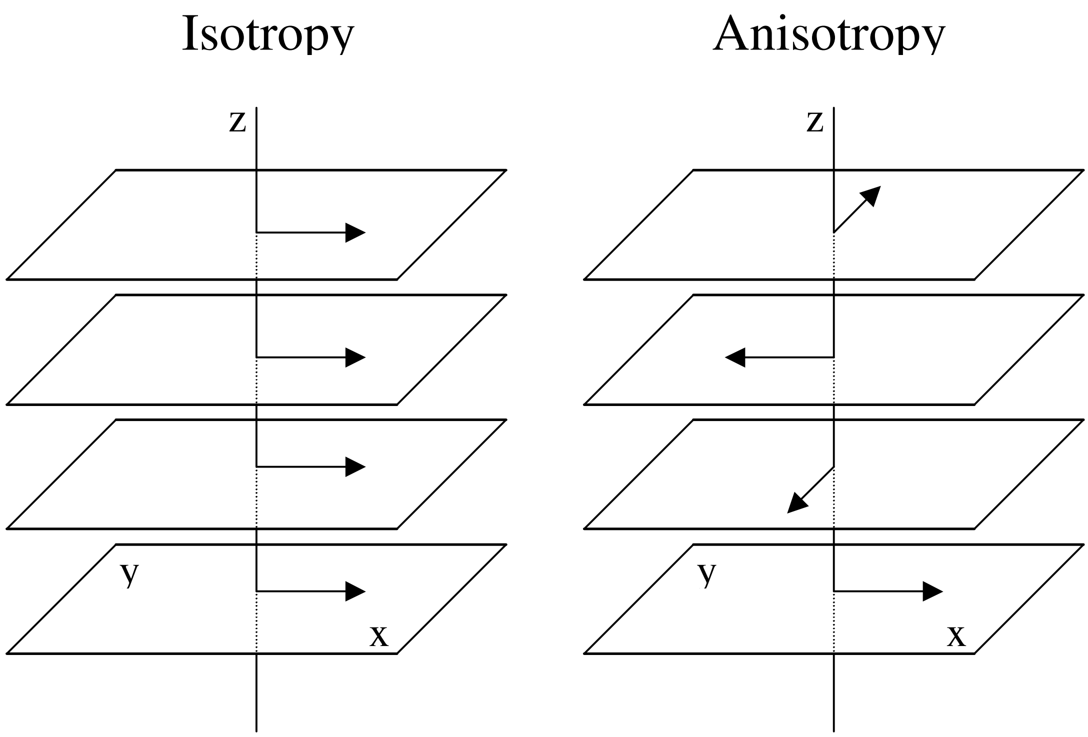

Figure 2. Ray-theoretical polarizations of a plane *S* wave propagating along the *z*-axis in an isotropic medium (left) and in an anisotropic medium with a rotating axis of symmetry (right).

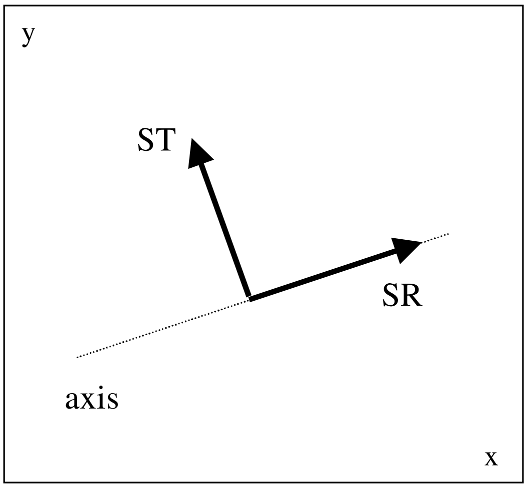

Figure 3. Definition of *SR* and *ST* waves. Dashed line: projection of the symmetry axis of the medium into the x-y plane.

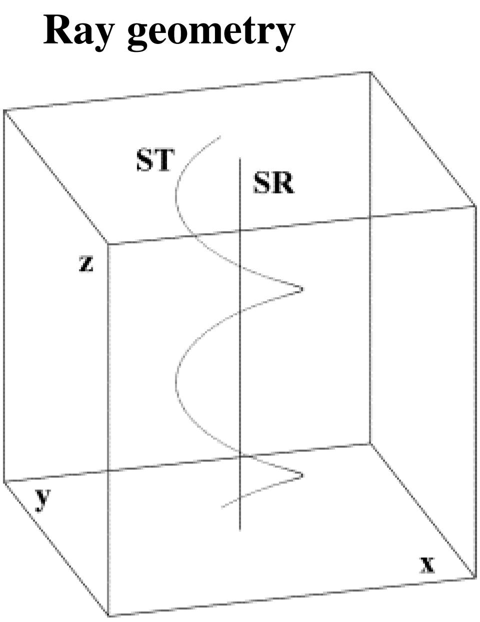

Figure 4. Geometry of rays of the *SR* and *ST* waves.

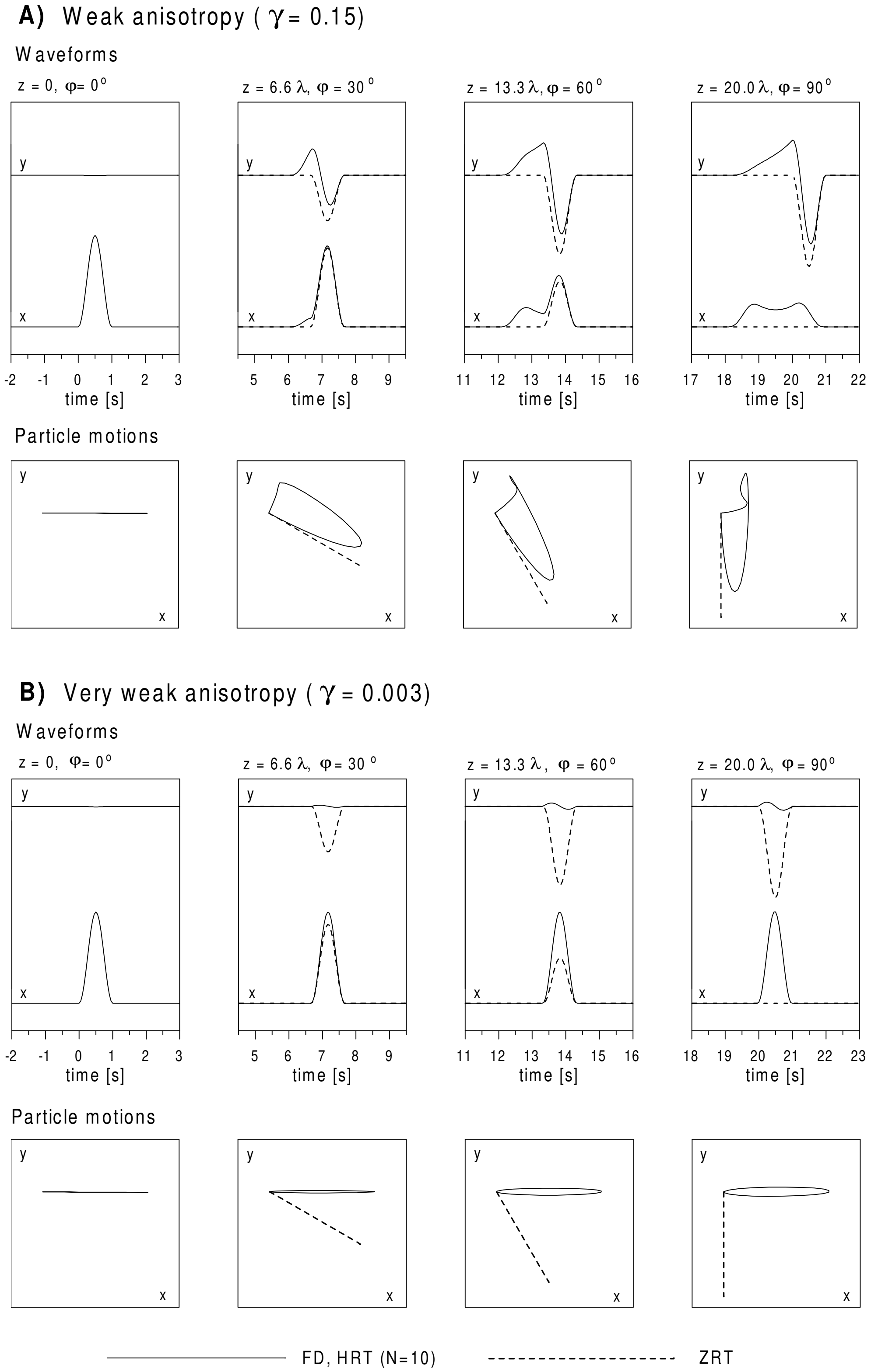

Figure 5. Waveforms and particle motions of the *S* wave propagating in weak (A) and very weak (B) anisotropy models. Diagrams are shown for four receivers with positions at $z = 0, 6.6\lambda^{SR}, 13.3\lambda^{SR}$ and $20.0\lambda^{SR}$, where $\lambda^{SR} = 2.45$ km. The rate of symmetry axis rotation is $b = \varphi / z = \pi / 40\lambda^{SR} = 0.032$. Full line: FD solution and/or RT solution with 10 higher-order approximations. Dashed line: the zeroth-order RT solution.

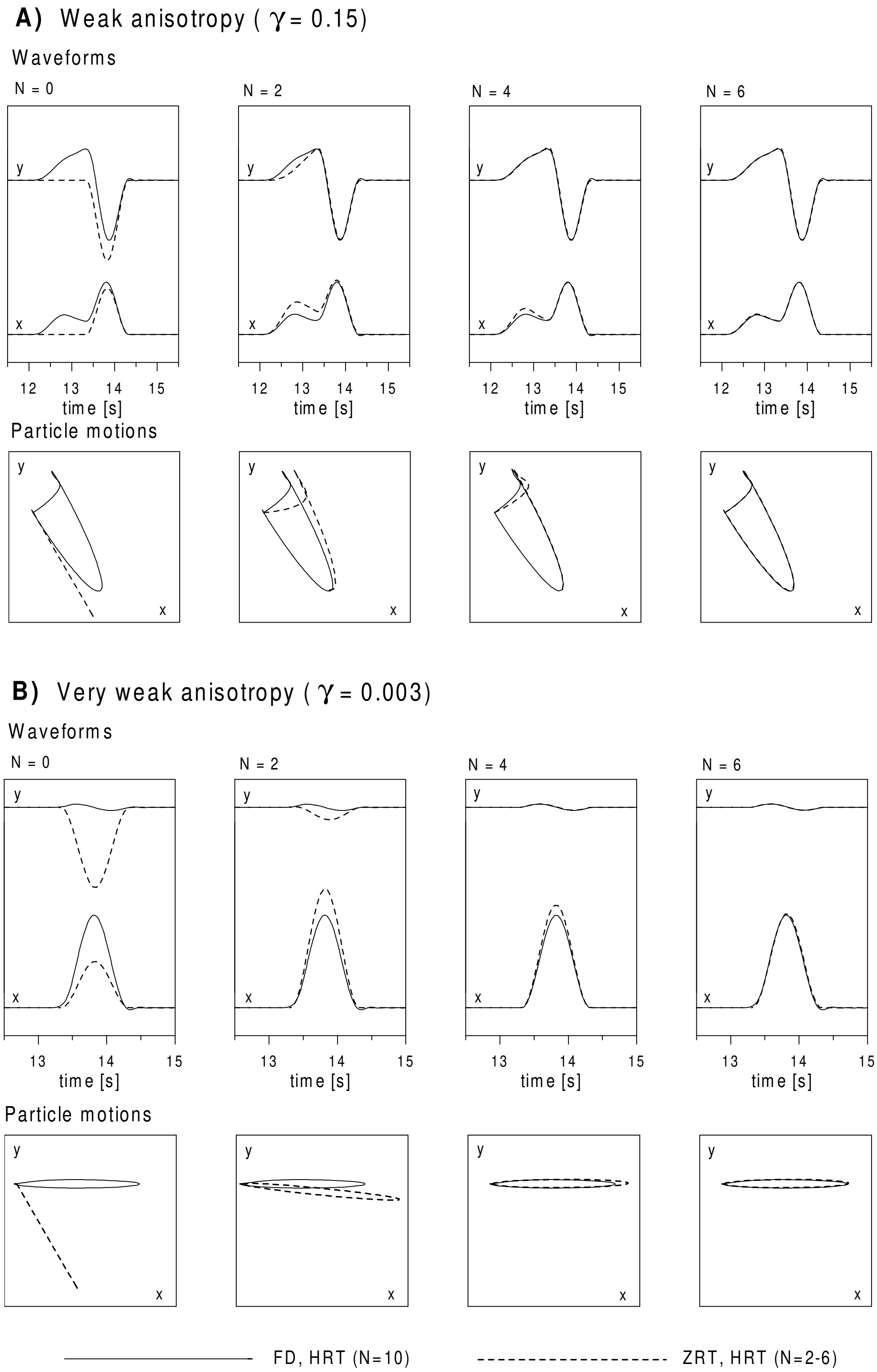

Figure 6. Waveforms and particle motions of the *S* wave propagating in weak (A) and very weak (B) anisotropy models. The receiver is at $z = 13.3\lambda^{SR}$ and the rate of rotation is $b = \pi / 40\lambda^{SR} = 0.032$. Diagrams are shown for RT solutions with a different number of higher-order approximations: *N*=0, 2, 4 and 6 (dashed line). Full line: FD solution and/or RT solution with 10 higher-order approximations.

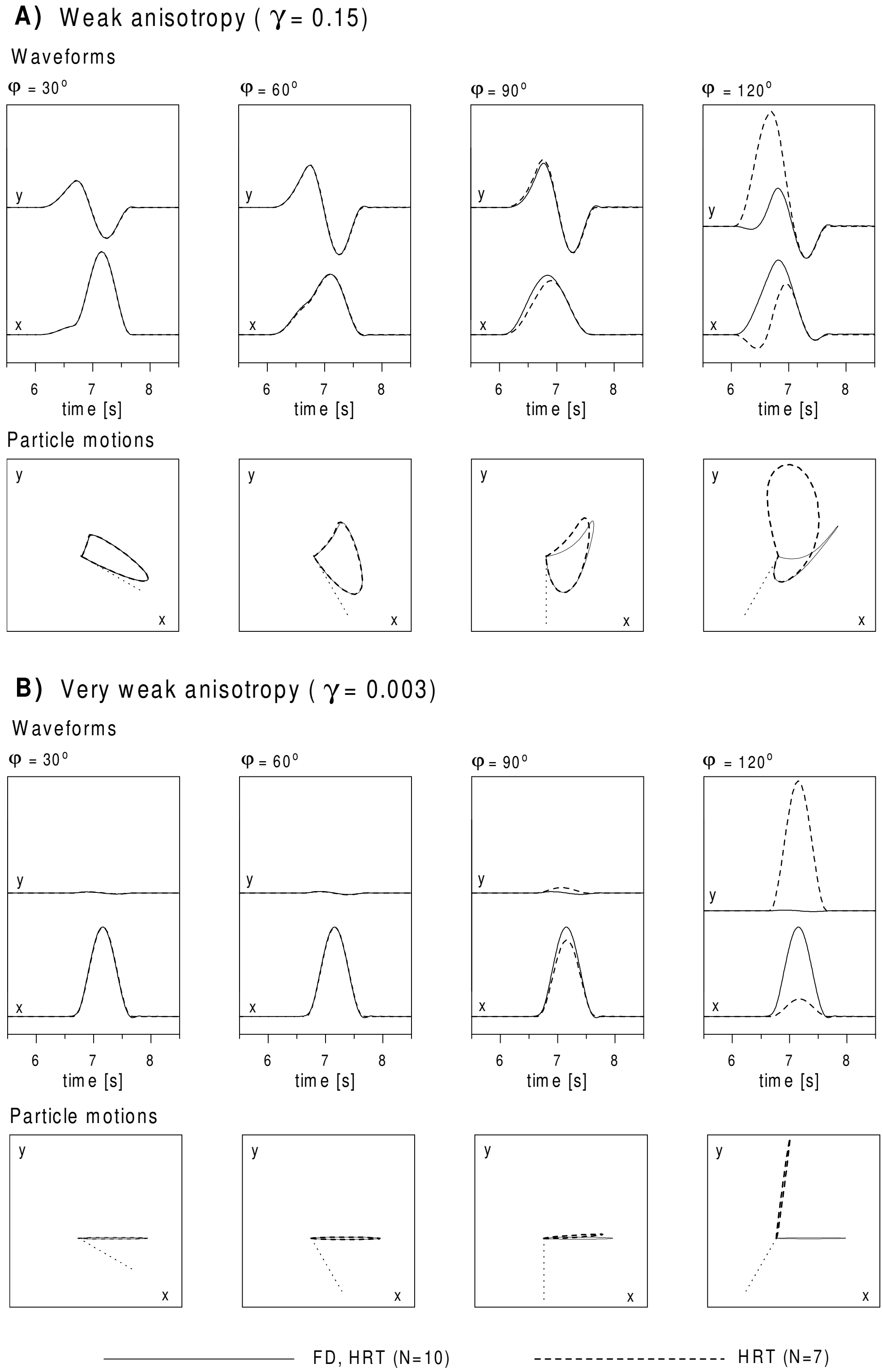

Figure 7. Waveforms and particle motions of the S wave propagating in weak (A) and very weak (B) anisotropy models. The receiver is at $z = 6.6\lambda^{SR}$. Diagrams are displayed for the rates of rotation (from left to right): $b = \pi / 40\lambda^{SR}, 2\pi / 40\lambda^{SR}, 3\pi / 40\lambda^{SR}$ and $b = 4\pi / 40\lambda^{SR}$. Full line: FD solution and/or RT solution with 10 higher-order approximations. Dashed line: RT solution with 7 higher-order approximations. Dotted line: projection of the symmetry axis into the *x-y* plane.